# Murine leukemia virus glycosylated Gag (gPr80$^{gag}$) facilitates interferon-sensitive virus release through lipid rafts

Takayuki Nitta, Yurii Kuznetsov, Alexander McPherson, and Hung Fan[1]

Department of Molecular Biology and Biochemistry, and Cancer Research Institute, University of California, Irvine, CA 92697-3905

Edited by Stephen P. Goff, Columbia University College of Physicians and Surgeons, New York, NY, and approved November 30, 2009 (received for review July 31, 2009)

**Murine leukemia viruses encode a unique form of Gag polyprotein, gPr80$^{gag}$ or glyco-gag. Translation of this protein is initiated from full-length viral mRNA at an upstream initiation site in the same reading frame as Pr65$^{gag}$, the precursor for internal structural (Gag) proteins. Whereas gPr80$^{gag}$ is evolutionarily conserved among gammaretroviruses, its mechanism of action has been unclear, although it facilitates virus production at a late assembly or release step. Here, it is shown that gPr80$^{gag}$ facilitates release of Moloney murine leukemia virus (M-MuLV) from cells along an IFN-sensitive pathway. In particular, gPr80$^{gag}$-facilitated release occurs through lipid rafts, because gPr80$^{gag}$-negative M-MuLV has a lower cholesterol content, is less sensitive to inhibition of release by the cholesterol-depleting agent MβCD, and there is less Pr65$^{gag}$ associated with detergent-resistant membranes in mutant-infected cells. gPr80$^{gag}$ can also facilitate the release of HIV-1-based vector particles from human 293T cells.**

Moloney | HIV-1 | BST-2/tetherin | retrovirus

Murine leukemia viruses (MuLVs) are prototypical simple retroviruses and they carry three genes, *gag*, *pol*, and *env*, that encode the viral core proteins, enzymes, and envelope proteins, respectively. One unique feature of MuLVs and many other gammaretroviruses is that they encode an additional form of Gag polyprotein, gPr80$^{gag}$, and a corresponding Gag-Pol polyprotein. gPr80$^{gag}$ is translated from unspliced viral mRNA via an upstream CUG initiation codon in the same reading frame as the Pr65$^{gag}$ precursor for viral core proteins (1–3). gPr80$^{gag}$ contains 88 additional amino-terminal amino acids, including a signal peptide that leads to transport of the protein into the rough endoplasmic reticulum, where it is glycosylated and exported to the cell surface (4) and cleaved into two proteins of ≈55 and 40 kDa (1, 5); the amino-terminal protein is reinserted through the plasma membrane, with the N-terminal unique sequences exposed to the cytoplasm (4).

gPr80$^{gag}$'s is conserved among gammaretroviruses, but its mechanism of action has been elusive. MuLVs mutant in gPr80$^{gag}$ are replication-competent with minor reductions in infectivity *in vitro* (6). However, when infected into mice, there is strong *in vivo* selection for recovery of gPr80$^{gag}$ expression (7–9). gPr80$^{gag}$ also is a major pathogenic determinant for a neurotropathic MuLV recombinant, FrCasE (10–12). We recently showed that gPr80$^{gag}$ plays a role in a late step in viral assembly or release. gPr80$^{gag}$-negative MuLVs budding from cells show aberrant tube-like structures (9, 13). Expression of gPr80$^{gag}$ increases virus particle release without affecting the rate of gag protein synthesis, and the tube-like structures are replaced by typical spherical particles (9).

In this article, we describe a molecular function for gPr80$^{gag}$. gPr80$^{gag}$ facilitates Moloney MuLV (M-MuLV)-efficient release through cholesterol-rich lipid rafts.

## Results

**gPr80$^{gag}$ Renders M-MuLV Release Sensitive to IFN.** Recently a cellular factor BST-2/tetherin has been found to inhibit release of HIV-1 particles from cells, and this molecule is inducible by IFN (14). MuLV infection also is blocked by IFN at a very late stage in infection, with accumulation of virus particles at the cell surface (15, 16). Thus, IFN may block MuLV infection by induction of BST-2. Because gPr80$^{gag}$ facilitates virus release, we hypothesized that gPr80$^{gag}$ may counteract inhibitory effects of BST-2. Thus gPr80$^{gag}$-negative virus might be more sensitive to IFN than wild-type M-MuLV.

17-5 cells are NIH 3T3 cells infected with a gPr80$^{gag}$-negative mutant M-MuLV (6, 17). We compared the effects of IFN on virus release into the media from 17-5 cells vs. wild-type M-MuLV-infected NIH 3T3 cells (43D) after 24 h of IFN-α treatment (Fig. 1 *A* and *B*). In the absence of IFN, 43D cells released approximately twice as much virus as 17-5 cells, consistent with gPr80$^{gag}$ facilitating virus release. Release of wild-type M-MuLV from 43D cells was potently inhibited by IFN, with 98–99% inhibition at maximal doses. The virus remained cell-associated, as indicated by cell-associated cleaved CA$^{p30}$ capsid protein. In contradiction to our initial hypothesis, release of virus from 17-5 cells was largely resistant to IFN and there was little build-up of cell-associated virus. The difference between IFN inhibition of virus release from 17-5 and 43D cells did not reflect differential induction of BST-2 (Fig. S1). The differential sensitivities very likely reflected the gPr80$^{gag}$ state of the viruses because NIH 3T3 cells freshly infected with viruses from 43D vs. 17-5 cells showed the same differential response to IFN (Fig. S2). Atomic force microscopy confirmed the accumulation of spherical virus particles on the surface of IFN-treated 43D cells, whereas there were less effects on the 17-5 cells (Fig. S3).

We previously showed that release of viral vector particles from the amphotropic MuLV-based packaging line PA317 (gPr80$^{gag}$-negative) is also greatly enhanced by expression of gPr80$^{gag}$ (9). We compared IFN-treated PA317 cells stably expressing an M-MuLV-based β-gal vector and a gPr80$^{gag}$ expression plasmid (PA317/BAG/p8065), with the same cells expressing the vector only (PA317/BAG/ΔMCS) (9). The gPr80$^{gag}$-expressing PA317 cells released vector particles substantially more efficiently (8-fold more) than the control packaging cells in the absence of IFN (Fig. 1 *C* and *D*). The release of vector particles from PA317/BAG/p8065 was strongly inhibited by IFN, whereas release from the control packaging cells was resistant (Fig. 1 *C* and *D*). The results of Figs. 1, S1, and S2 suggested that M-MuLV can be released from infected cells by two pathways—one IFN-sensitive and one IFN-resistant—and that gPr80$^{gag}$ may direct assembly/release toward the IFN-sensitive pathway.

Author contributions: H.F. designed research; T.N. and Y.K. performed research; A.M. contributed new reagents/analytic tools; and T.N. and H.F. wrote the paper.

The authors declare no conflict of interest.

This article is a PNAS Direct Submission.

[1]To whom correspondence should be addressed. E-mail: hyfan@uci.edu.

This article contains supporting information online at www.pnas.org/cgi/content/full/0908660107/DCSupplemental.

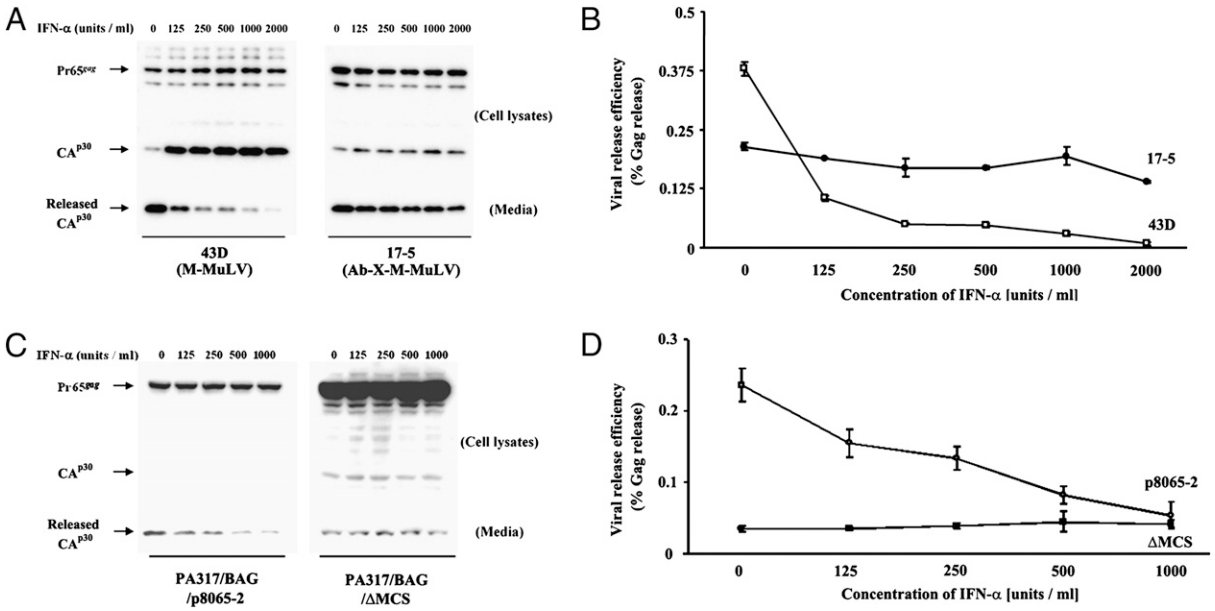


**Fig. 1.** Effect of IFN-α on virus release from 43D and 17-5 cells. (*A*) 43D and 17-5 cells were treated with different concentrations of mouse IFN for 24 h, after which media were replaced and the cells and released viruses were collected 6 h after incubation. The same portions of cells and released viruses were subjected to the Western blots with anti-$CA^{p30}$. (*B*) Virus release efficiency from 43D and 17-5 cells was calculated (means ± SD from three replicate experiments). (*C* and *D*) PA317/BAG/ΔMCS and PA317/BAG/p8065-2 cells were analyzed as in *A* and *B*.

**$gPr80^{gag}$ Facilitates Viral Release Through Lipid Rafts.** We next tested whether $gPr80^{gag}$ might facilitate M-MuLV release through cholesterol-rich plasma membrane subdomains, also called lipid rafts. HIV buds through lipid rafts (18, 19), and this process has also been reported for MuLV (20, 21). BST-2 localizes in lipid rafts (22), so IFN induction of BST-2 would be expected to efficiently inhibit release of virions budding through lipid rafts, whereas it would be expected to have less effect on virus released independent of lipid rafts. We compared the cholesterol content of purified wild-type and $gPr80^{gag}$-negative viruses. Viruses from 43D and 17-5 cells and from NIH 3T3 cells freshly infected with wild-type and Ab-X-M-MuLV were purified by buoyant density gradient centrifugation and analyzed for cholesterol content. To control for released vesicles in the preparations, the equivalent gradient fractions from supernatants of uninfected NIH3T3cells were analyzed for cholesterol content and the values were subtracted from those for the viruses. The cholesterol content of virus released from 17-5 or 3T3/Ab-X-M-MuLV cells was significantly less (2.3- to 2.5-fold less) compared to virus from 43D or 3T3/WT-M-MuLV cells (Table 1), consistent with $gPr80^{gag}$ directing budding through lipid rafts.

If $gPr80^{gag}$ directs viral budding through lipid rafts then the $Pr65^{gag}$ precursor for the viral core proteins might show higher association with lipid rafts in wild-type vs. $gPr80^{gag}$-negative M-MuLV-infected cells. Lipid rafts (also known as detergent resistant membranes or DRMs) are resistant to nonionic detergents, so membrane flotation assays on cytoplasmic extracts prepared in 1% Triton X-100 were performed (Fig. 2*A*). As predicted, ≈15% of $Pr65^{gag}$ was associated with DRMs from 43D cells, whereas ≈5% (3-fold less) was in DRMs from 17-5 cells. Interestingly the majority of $gPr80^{gag}$ itself was not in the DRMs (Fig. 2*A*).

We also employed confocal microscopy to study the membrane localization of Gag protein in 43D and 17-5 cells. Cells grown on coverslips were incubated at 4 °C with either saline or 0.5% Triton X-100, which would dissolve the membranes except for DRMs. The cells were then fixed with paraformaldehyde, followed by immunofluorescent staining. As expected, staining for the non-DRM-associated plasma membrane protein CD71 was found at the plasma membrane/outline of the cells (as well as internally) in cells incubated with PBS; this staining was dispersed by treatment with detergent (23) (Fig. S4). In contrast, staining for the DRM/lipid raft protein Caveolin showed plasma membrane (and internal) localization that was resistant to detergent treatment (Fig. S4). Staining for M-MuLV Gag protein with anti-$CA^{p30}$ antibody showed diffuse and punctate cytoplasmic staining as well as staining at the plasma membrane for both 43D and 17-5 cells in the absence of detergent (Fig. 2*B a* and *c*). Whereas staining at the plasma membrane was still detectable after detergent treatment for 43D cells (Fig. 2*Bb*), detergent-treated 17-5 cells showed no localization at the plasma membrane. The absence of Gag at the plasma membrane in 17-5 cells was consistent with Fig. 2*A*, in which substantially more $Pr65^{gag}$ was associated with DRMs in 43D vs. 17-5 cells. The anti-Gag staining in Fig. 2*B* visualized both $Pr65^{gag}$ and $gPr80^{gag}$ and their cleavage products. Because $gPr80^{gag}$ is not associated with DRMs (Fig. 2*A*), detergent treatment would be expected to remove it from the plasma membrane.

**Table 1. Relative cholesterol in viral particles released from WT-M-MuLV- and Ab-X-M-MuLV-infected cells**

| Cells | Cholesterol contents in WT-M-MuLV/Ab-X-M-MuLV |
|---|---|
| 43D vs. 17-5 | |
| Exp 1 | 2.240 |
| Exp 2 | 2.352 |
| Exp 3 | 2.411 |
| Ave | 2.334 ± 0.087 |
| 3T3/WT-M-MuLV vs. 3T3/Ab-X-M-MuLV | |
| Exp 1 | 2.548 |
| Exp 2 | 2.496 |
| Ave | 2.522 ± 0.037 |

The ratios of the cholesterol contents in virus released from WT- and Ab-X-M-MuLV–infected cells are shown. Detailed data and calculations are described in Table S1 and *Materials and Methods*. The differences in cholesterol contents between 43D and 17-5 ($P < 0.005$) and between 3T3/WT-M-MuLV and 3T3/Ab-X-M-MuLV ($P < 0.05$) viruses were significant by Welch's twotailed *t* test.

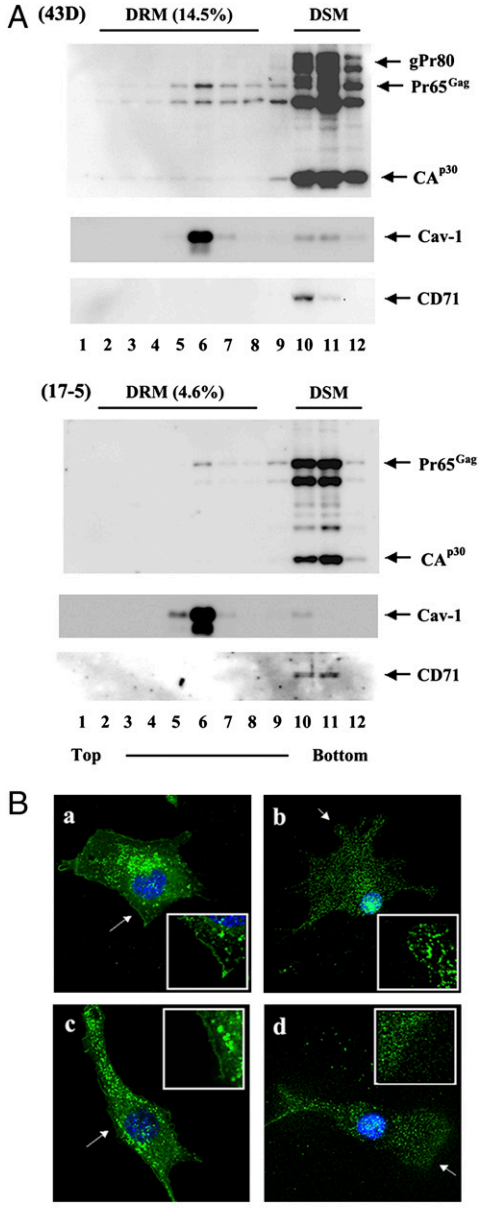


**Fig. 2.** Differential Gag localization in lipid rafts. (*A*) Lysates (1% Triton X-100) from 43D and 17-5 cells were analyzed by membrane flotation in 5–30% sucrose gradients. Low-density fractions represented detergent-resistant membranes (DRMs)/lipid rafts, whereas high-density fractions represented protein in detergent-soluble membranes (DSMs) or cytosolic proteins. Gradient fractions were analyzed by Western blots for viral $CA^{p30}$, Caveolin (lipid rafts marker), and CD-71 (nonlipid rafts marker). The amount of $Pr65^{gag}$ was quantified by densitometry. The percentage of $Pr65^{gag}$ in lipid rafts is shown in parentheses. The band migrating more rapidly than $Pr65^{gag}$ represents a partial proteolytic cleavage product. There are two bands corresponding to $gPr80^{gag}$ (absent from 17-5 cells) that correspond to different states of glycosylation. (*B*) 43D cells (*a* and *b*) and 17-5 cells (*c* and *d*) were incubated with ice-cold PBS (*a* and *c*) or 0.5% Triton X-100 (*b* and *d*) followed by fixation with paraformaldehyde and then incubation with anti-$CA^{p30}$ antibody. The antigens and nuclei were visualized by secondary antibodies conjugated with Alexa 488 and DAPI (to visualize the nuclei). The regions indicated by arrows were enlarged in the insets.

**Depletion of Cholesterol Impairs Wild-Type M-MuLV Release.** To assess whether association of Gag with lipid rafts is important for virus release, we used methyl-beta-cyclodextrin (MβCD) to extract cholesterol from plasma membranes of infected cells (24). 43D and 17-5 cells were treated for 30 min with MβCD at various concentrations and virus release was measured (Fig. 3 *A* and *B*). Increasing concentrations of MβCD reduced virus release from 43D cells, with ≈50% reduction at the maximal concentration—similar to effects of MβCD on HIV-1 release (18). In contrast, release of virus from 17-5 cells was not affected by MβCD.

In our original characterization of $gPr80^{gag}$-negative M-MuLV, we noticed that it had a slightly higher buoyant density than wild-type virus (6). We tested whether the density difference reflected differential cholesterol contents and/or budding through lipid rafts. In Fig. 3*C*, virus from 43D cells had a density of 1.161 g/cc, whereas $gPr80^{gag}$-gag negative virus from 17-5 cells showed a higher density of 1.170 g/cc. Similarly, $gPr80^{gag}$-negative virus from freshly infected NIH 3T3 cells and 293T cells transiently transfected with M-MuLV packaging plasmid expressing Gag-Pol proteins had a higher density than wild-type M-MuLV and M-MuLV Gag-Pol coexpression with $gPr80^{gag}$ (Fig. S5). Moreover, virus released from MβCD-treated 43D cells had a buoyant density of 1.175 g/cc, similar to the density of $gPr80^{gag}$-negative virus from 17-5 cells. Virus from MβCD-treated 17-5 cells also showed an increase in density to 1.177 g/cc, although the densities of virus from the two MβCD-treated cells were similar.

**$gPr80^{gag}$ Facilitates Release of a Heterologous Virus.** Finally, we tested whether MuLV $gPr80^{gag}$ can facilitate release of the other retroviruses. We cotransfected 293T cells with an HIV-1 packaging plasmid expressing Gag-Pol proteins along with the $gPr80^{gag}$ expression plasmid p8065-2 and assessed viral release efficiency. As shown in Fig. 4*A Middle*, the amount of released virions ($CA^{p24}$ protein in the supernatant) was greatly enhanced by coexpression of $gPr80^{gag}$. Interestingly, this enhancement reflected both an increase in the amount of HIV-1 Gag-pol ($Pr55^{gag}$) in the cells (Fig. 4 *A Upper* and *B*), as well as the efficiency of virus release after correction for amount of Gag-pol synthesized (Fig. 4*C*). $gPr80^{gag}$ enhanced release of HIV-1 particles by 6- to 10-fold, a similar magnitude of enhancement compared to MuLV (9) (Fig. S6). The enhancement of particle release did not depend on the presence of HIV-1 and M-MuLV Env proteins.

## Discussion

In these experiments, we describe a mechanism for the function for the $gPr80^{gag}$ protein of M-MuLV: direction of virus release through lipid rafts. This was first identified by the differential sensitivity of cells infected with wild-type (43D) and $gPr80^{gag}$-negative M-MuLV (17-5) to treatment with IFN, which indicated that $gPr80^{gag}$ directs virus release through an IFN-sensitive pathway. This pathway involves release through lipid rafts because wild-type virus showed a higher cholesterol content, DRMs from wild-type-infected cells showed higher amounts of the $Pr65^{gag}$ polyprotein precursor, and depletion of cholesterol from lipid rafts by MβCD reduced release of wild-type but not $gPr80^{gag}$-negative M-MuLV.

The fact that 17-5 cells release virus less efficiently than 43D cells indicates that virus release through lipid rafts is more efficient than through other membrane structures/regions. Perhaps concentration of $Pr65^{gag}$ facilitates multimerization and viral assembly. Virus budding from $gPr80^{gag}$-negative cells tends to be in the form of elongated "tubes" as opposed to spherical virions (9, 13). Thus, the tubes may represent budding through nonlipid rafts. In fact, some of the viruses released from 17-5 cells might also bud through lipid rafts (i.e., the low level of $Pr65^{gag}$ in DRMs in these cells), although the relative frequency is much lower than for 43D cells. Indeed, spherical particles were observed on the surface of 17-5 cells in addition to tubes (Fig. S3).

The mechanism by which $gPr80^{gag}$ directs virus budding to lipid rafts remains to be determined. The process results in association of $Pr65^{gag}$ with DRMs, but it does not require viral

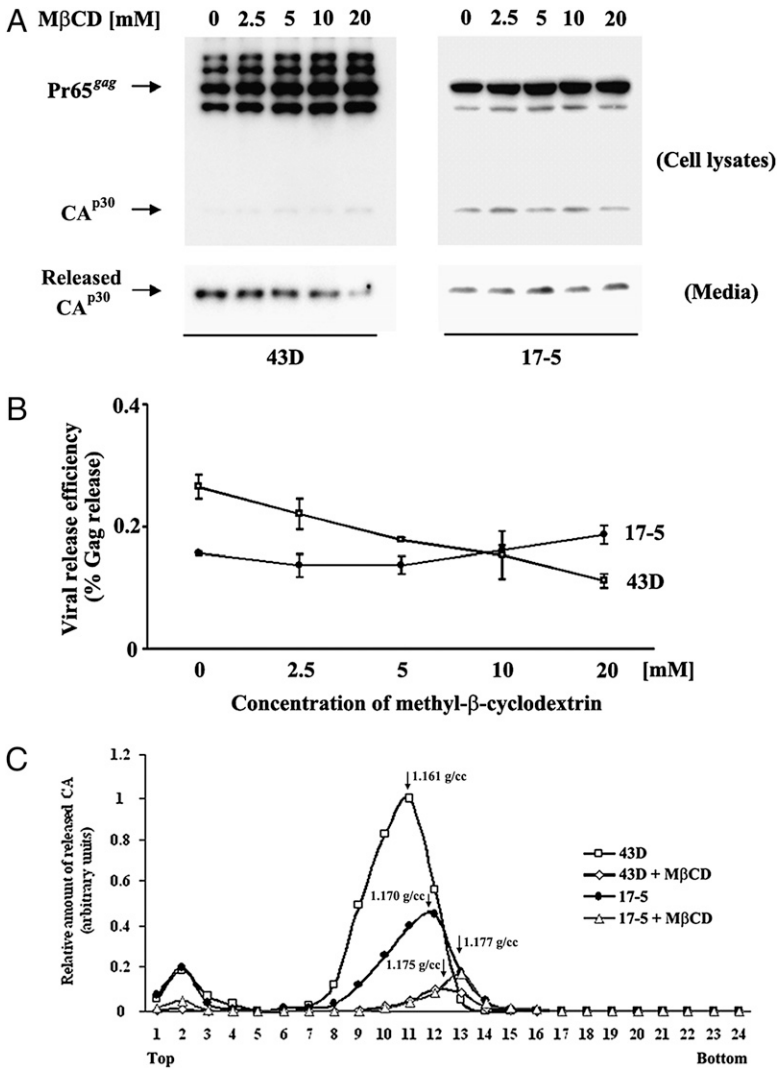


**Fig. 3.** MβCD impairment of viral release. (*A*) 43D and 17-5 cells were treated with different concentrations of MβCD and the amount of virus release after 6 h was assayed as in Fig. 1. (*B*) Viral release efficiencies from 43D and 17-5 cells were calculated as in Fig. 1 (means of two experiments ± SD). (*C*) 43D and 17-5 cells were incubated with or without 5 mM MβCD for 12 h. Viruses were harvested and analyzed by density gradient centrifugation, and distribution of $CA^{p30}$ was analyzed by Western blots and densitometry. The lower amounts of virus released from the MβCD-treated cells likely reflected cell toxicity after longer incubation in MβCD and serum-free medium.

Env protein. The majority of $gPr80^{gag}$ is not localized to lipid rafts; thus, it might be interacting with a cellular protein that conducts $Pr65^{gag}$, which is largely membrane-associated through N-terminal myristilation, to the lipid rafts.

In vivo, $gPr80^{gag}$ could be particularly important for virus release from cells that have prominent and well-developed lipid rafts. T lymphocytes form highly organized immunological synapses upon contact with antigen-presenting cells or other immune cells, and lipid rafts are important in formation of these synapses (25, 26). Moreover, HIV-1 can spread from infected T lymphocytes to other cells by direct contact through virological synapses that result from viral adaptation of the immunological synapses (27). MuLVs generally infect hematopoietic cells *in vivo*, and M-MuLV predominantly infects T lymphocytes. Thus, $gPr80^{gag}$ could be directing M-MuLV release through immunological/virological synpses in those cells. Release through these synapses could explain why $gPr80^{gag}$-negative M-MuLV shows a stronger defect in mice than in fibroblasts *in vitro*.

As shown in Fig. 4, $gPr80^{gag}$ can also facilitate release of a heterologous retrovirus particle containing *gag-pol* of HIV-1. In 293T cells, the enhancement of HIV-1 particle production included both enhanced release as well as enhanced production of Gag polyprotein. The mechanisms are under investigation, and our current hypothesis is that $gPr80^{gag}$ is at least facilitating release of HIV-1 particles through lipid rafts. We have also observed that $gPr80^{gag}$ enhances release of jaagsiekte sheep retrovirus (JSRV, a betaretrovirus) by ≈2-fold (G. Luo, T. Nitta, and H. Fan, unpublished data). Enhancement of HIV-1 particle release by MuLV glyco-gag may be of interest to those interested in generating high titer lentiviral vectors.

Very recently another investigator has also observed an effect of $gPr80^{gag}$ on retrovirus release consistent with this report (M. Pizzato, personal communication). Nef-deleted HIV-1 shows a release defect in human T-lymphoid cell lines, and this defect could be complemented by MuLV $gPr80^{gag}$. This effect was predominantly observed in T lymphocytes and not in other cell types. Others have reported that Nef-negative HIV-1 has a lower cholesterol content (28), consistent with a role for Nef in directing virus release through lipid rafts, and with $gPr80^{gag}$ being able to carry out the same process.

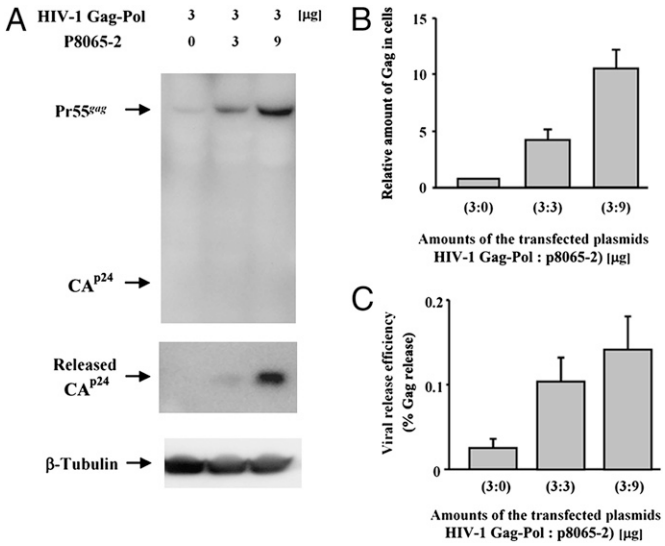


**Fig. 4.** gPr80$^{gag}$ increases the efficiency of HIV-1 particle release. The HIV-1 Gag-Pol expression vector was transfected with or without p8065-2 into 293T cells. (*A*) The cells and media were harvested 48 h after transfection, and the same portions of cells and viruses were analyzed by Western blots with anti-HIV CA$^{p24}$ and anti-β-Tubulin antibodies. The relative amounts of Gag (*B*) in cells and viral release efficiencies (*C*) were quantified (means of two experiments, ±SD).

## Materials and Methods

**Reagents and DNA Constructs.** The plasmid p8065-2 expressing MuLV gPr80$^{gag}$ was described in ref. 9. For assessment of viral release from the cells transiently transfected with retroviral constructs encoding *gag* and *pol* regions, gPr80$^{gag}$-negative M-MuLV Gag-Pol expression vector, AKAQ188 and the HIV-1-based packaging vector pCMV-dR8.74 were used.

**Cells and Viruses.** 43D and 17-5 cells are NIH 3T3 fibroblasts stably infected with wild-type and gPr80$^{gag}$-negative Ab-X-M-MuLV, respectively (6, 17). The cells were from low passage numbers after establishment (<20). PA317/BAG/ΔMCS and PA317/BAG/8065–2 cells are PA317 amphotropic MuLV-based packaging cells stably transfected with an M-MuLV-based vector (BAG) expressing bacterial β-gal with or without p8065-2 (9).

**Antibodies and Chemicals.** Rabbit polyclonal anti-MuLV CA$^{p30}$ antisera were described in ref. 29. Mouse monoclonal anti-HIV-1 CA$^{p24}$ antibodies (YDHIVgp24) were purchased from MyBioSource. Rabbit polyclonal antibodies against Caveolin-1 (BD Biosciences) and CD71 (Santa Cruz Biotechnology) and mouse anti-CD71 (H68.4: Zymed Laboratories) antibodies were used. For Western blots, we used anti-mouse IgG conjugated with horseradish peroxidase (Thermo Scientific) and anti-rabbit IgG conjugated with horseradish peroxidase (GE Healthcare). For indirect fluorescence microscopy, anti-mouse and anti-rabbit IgG conjugated with Alexa 488 (Invitrogen) were used. Mouse IFN-α (IFN) and methyl-beta-cyclodextrin (MβCD) were purchased from Calbiochem and Sigma, respectively.

**IFN Treatment and Virus Release.** The virus-infected or vector-producing cells were seeded on 6-cm dishes the day before and then treated with the different doses of IFN for 24 h, and then media were replaced. The cells and media were harvested after 6–8 h further incubation. The media were clarified by low-speed centrifugation, passed through a 0.45-μm filter and viral particles were pelleted in a Beckman SW41 rotor at 77,000 × *g* for 1 h. The pelleted viral particles and corresponding cell lysates were analyzed by SDS/PAGE and Western blots using anti-MuLV CA$^{p30}$. To quantify viral release, each Pr65$^{gag}$ and CA$^{p30}$ band in the cells and media was quantified with the densitometry software AlphaEaseFC (Alpha Innotech), and the percentage of released CA$^{p30}$ divided by total Gag proteins (Pr65$^{gag}$ and CA$^{p30}$) in cells and media was calculated. Different exposures of the blots were analyzed to ensure that densitometry was in the linear range.

**Virus Purification and Cholesterol Determination.** Viral particles were harvested from cell supernatants by pelleting as described above, followed by suspension in 400 μL of NTE buffer containing 10 mM Tris·HCl (pH 7.4), 100 mM NaCl, 1 mM EDTA, and layered on a 20–55% (wt/vol) linear sucrose gradient made in NTE buffer. After centrifugation in an SW41 rotor at 150,000 × *g* for 18 h, the gradients were fractionated and fractions were analyzed by Western blots with anti-MuLV CA$^{p30}$.

To quantify cholesterol, sucrose gradient fractions with banded virus or the equivalent fractions from uninfected NIH 3T3 cells were pooled, diluted with NTE buffer, virus was pelleted by ultercentrifugation, and the pellets were suspended in NTE buffer. The virus-producing cells were lysed in 0.1 M potassium phosphate (pH 7.4), 0.25 M NaCl, 25 mM cholic acid, 0.5% Triton X-100. The amount of cholesterol in viruses and cell lysates were determined by the Amplex Red Cholesterol Assay Kit (Invitrogen). For normalization the amounts of viruses were quantified by Western blots using anti-MuLV CA$^{p30}$ and total cellular proteins by the Dc Protein Assay Kit (Bio-Rad).

**Treatment of Cells with MβCD.** 43D and 17-5 cells were seeded on 6-cm dishes the day before MβCD treatment. The cells were washed in PBS twice and incubated for 1h in serum-free DMEM, incubated for 30 min at 37 °C in serum-free DMEM containing different concentrations of MβCD, washed three times with PBS followed by replacement with growth medium. The cells and media were gathered after 6 h and subjected to Western blots. For sucrose density gradient analysis, the cells were incubated with 5 mM MβCD in serum-free DMEM for 12 h. Virus from the supernatants was harvested and analyzed in sucrose density gradient as described above.

**Confocal Microscopy.** Confocal microscopy was described in ref. 13 and in *SI Text*.

**Flotation of DRM Domains.** Flotation of DRM was performed as described in ref. 30 with slight modifications. 43D and 17-5 cells were treated on the dish with lysis buffer (0.8 mL/10 cm dish) containing 25 mM Tris·HCl (pH 8.0), 140 mM NaCl, 1% Triton X-100, 1 mM EDTA, 1 mM PMSF, 1 mM $Na_3VO_4$, and protease inhibitor mixture (Roche) for 20 min at 4 °C. The lysates were harvested and then centrifuged at 10,000 × *g* for 5 min at 4 °C. The postnuclear lysate was adjusted to 40% (wt/vol) sucrose, and then a 5–30% discontinuous sucrose gradient was layered on the top. Samples were centrifuged at 100,000 × *g* for 18–24 h at 4 °C. The fractions were collected from the top of the gradient tube. The Western blot analysis was performed to identify the fractions containing lipid raft and nonlipid raft domains.

**ACKNOWLEDGMENTS.** We thank Guopei Luo, Raymond Tam, Alexander Hamil, and Kerry Fitzgerald for assistance and participation in experiments, and the Optical Biology Shared Resource of the Chao Family Comprehensive Cancer Center for confocal microscopy. The advice of Drs. Paul Bieniasz and David Camerini is appreciated. We are grateful to Dr. Lorraine Albritton for the gift of the M-MuLV plasmid encoding the *gag* and *pol* regions. This work was supported by NIH Grants CA94188 (to H.F.) and GM080412 (to A.M.).

1. Edwards SA, Fan H (1979) gag-Related polyproteins of Moloney murine leukemia virus: Evidence for independent synthesis of glycosylated and unglycosylated forms. *J Virol* 30:551–563.
2. Buetti E, Diggelmann H (1980) Murine leukemia virus proteins expressed on the surface of infected cells in culture. *J Virol* 33:936–944.
3. Prats AC, De Billy G, Wang P, Darlix JL (1989) CUG initiation codon used for the synthesis of a cell surface antigen coded by the murine leukemia virus. *J Mol Biol* 205:363–372.
4. Fujisawa R, McAtee FJ, Zirbel JH, Portis JL (1997) Characterization of glycosylated Gag expressed by a neurovirulent murine leukemia virus: identification of differences in processing in vitro and in vivo. *J Virol* 71:5355–5360.
5. Ledbetter J, Nowinski RC, Emery S (1977) Viral proteins expressed on the surface of murine leukemia cells. *J Virol* 22:65–73.
6. Fan H, Chute H, Chao E, Feuerman M (1983) Construction and characterization of Moloney murine leukemia virus mutants unable to synthesize glycosylated gag polyprotein. *Proc Natl Acad Sci USA* 80:5965–5969.
7. Chun R, Fan H (1994) Recovery of Glycosylated gag Virus from Mice Infected with a Glycosylated gag-Negative Mutant of Moloney Murine Leukemia Virus. *J Biomed Sci* 1:218–223.
8. Corbin A, Prats AC, Darlix JL, Sitbon M (1994) A nonstructural gag-encoded glycoprotein precursor is necessary for efficient spreading and pathogenesis of murine leukemia viruses. *J Virol* 68:3857–3867.
9. Low A, et al. (2007) Mutation in the glycosylated gag protein of murine leukemia virus results in reduced in vivo infectivity and a novel defect in viral budding or release. *J Virol* 81:3685–3692.
10. Fujisawa R, McAtee FJ, Wehrly K, Portis JL (1998) The neuroinvasiveness of a murine retrovirus is influenced by a dileucine-containing sequence in the cytoplasmic tail of glycosylated Gag. *J Virol* 72:5619–5625.
11. Portis JL, Fujisawa R, Mcatee FJ (1996) The glycosylated gag protein of MuLV is a determinant of neuroinvasiveness: Analysis of second site revertants of a mutant MuLV lacking expression of this protein. *Virology* 226:384–392.

12. Portis JL, Spangrude GJ, McAtee FJ (1994) Identification of a sequence in the unique 5′ open reading frame of the gene encoding glycosylated Gag which influences the incubation period of neurodegenerative disease induced by a murine retrovirus. *J Virol* 68:3879–3887.
13. Kuznetsov YG, et al. (2002) Atomic force microscopy investigation of fibroblasts infected with wild-type and mutant murine leukemia virus (MuLV). *Biophys J* 83: 3665–3674.
14. Neil SJ, Zang T, Bieniasz PD (2008) Tetherin inhibits retrovirus release and is antagonized by HIV-1 Vpu. *Nature* 451:425–430.
15. Chang EH, Mims SJ, Triche TJ, Friedman RM (1977) Interferon inhibits mouse leukaemia virus release: An electron microscope study. *J Gen Virol* 34:363–367.
16. Salzberg S, Bakhanashvili M, Aboud M (1978) Effect of interferon on mouse cells chronically infected with murine leukaemia virus: kinetic studies on virus production and virus RNA synthesis. *J Gen Virol* 40:121–130.
17. Hanecak R, Mittal S, Davis BR, Fan H (1986) Generation of infectious Moloney murine leukemia viruses with deletions in the U3 portion of the long terminal repeat. *Mol Cell Biol* 6:4634–4640.
18. Ono A, Freed EO (2001) Plasma membrane rafts play a critical role in HIV-1 assembly and release. *Proc Natl Acad Sci USA* 98:13925–13930.
19. Nguyen DH, Hildreth JE (2000) Evidence for budding of human immunodeficiency virus type 1 selectively from glycolipid-enriched membrane lipid rafts. *J Virol* 74: 3264–3272.
20. Pickl WF, Pimentel-Muiños FX, Seed B (2001) Lipid rafts and pseudotyping. *J Virol* 75: 7175–7183.
21. Li M, Yang C, Tong S, Weidmann A, Compans RW (2002) Palmitoylation of the murine leukemia virus envelope protein is critical for lipid raft association and surface expression. *J Virol* 76:11845–11852.
22. Kupzig S, et al. (2003) Bst-2/HM1.24 is a raft-associated apical membrane protein with an unusual topology. *Traffic* 4:694–709.
23. Beer C, Pedersen L, Wirth M (2005) Amphotropic murine leukaemia virus envelope protein is associated with cholesterol-rich microdomains. *Virol J* 2:36.
24. Francis SA, et al. (1999) Rapid reduction of MDCK cell cholesterol by methyl-beta-cyclodextrin alters steady state transepithelial electrical resistance. *Eur J Cell Biol* 78: 473–484.
25. Jury EC, Flores-Borja F, Kabouridis PS (2007) Lipid rafts in T cell signalling and disease. *Semin Cell Dev Biol* 18:608–615.
26. Simons K, Toomre D (2000) Lipid rafts and signal transduction. *Nat Rev Mol Cell Biol* 1: 31–39.
27. Campbell EM, Hope TJ (2008) Live cell imaging of the HIV-1 life cycle. *Trends Microbiol* 16:580–587.
28. Zheng YH, Plemenitas A, Fielding CJ, Peterlin BM (2003) Nef increases the synthesis of and transports cholesterol to lipid rafts and HIV-1 progeny virions. *Proc Natl Acad Sci USA* 100:8460–8465.
29. Mueller-Lantzsch N, Fan H (1976) Monospecific immunoprecipitation of murine leukemia virus polyribosomes: Identification of p30 protein-specific messenger RNA. *Cell* 9:579–588.
30. Radeva G, Sharom FJ (2004) Isolation and characterization of lipid rafts with different properties from RBL-2H3 (rat basophilic leukaemia) cells. *Biochem J* 380:219–230.